

Effect of Curing Time on Cell Structures

Yujing Zhao, Zuobin Wang*, Feng Hou

Yan Liu , Xinyue Wang, Yingmin Qu, Wenxiao Zhang

International Research Centre for Nano Handling & Manufacturing of China
Changchun University of Science and Technology, Changchun, China

Yan Liu

Changchun Medical College, Changchun, China

*Corresponding author: wangz@cust.edu.cn

Abstract—In this paper, the HL7702 cells were cured with 4% paraformaldehyde for different time durations. The atomic force microscope (AFM) and atomic force acoustic microscope (AFAM) were used to observe the surface and subsurface properties of the cured cells. The structures of the cells were changed with the curing time including the cytoskeleton, the shape, the height and the roughness of the cells. The lamellipodium can be seen for the curing time of 15 minutes with 4% paraformaldehyde. The optimal curing time was 15 minutes. This work provides a method for the study of cured cells in biomedicine.

Keywords—atomic force acoustic microscope; cell curing time; paraformaldehyde; acoustic image

I. INTRODUCTION

Cell is the basic unit of the living organisms [1]. There are many different types of cells in a human body. Every cell has the unique size, shape, structure and function. In recent years, studies have shown that cell structures play an important role in cell growth, differentiation, development, death and tumor growth. However, the cell structures are often changed in the curing process and will affect the study of cell properties. In this work, the cells were cured with 4% paraformaldehyde for different time durations. AFM and AFAM were used to observe the surface and subsurface characteristics which were changed with the cell structures.

AFM is a useful tool for the study of biological samples with nano resolution [2,3]. It works by the physical interaction of the cantilever tip with the molecules on the cell surface. The adhesion force between the tip and the cell surface molecule is measured as the cantilever deflection. Ohshiro et al. studied the direct neurite–mast cell (RBL) communication in vitro by AFM [4]. Kirmizis et al. measured the cell mechanics using an AFM [5]. Puech et al. provided a novel technological method to determine the cell-cell adhesion force based on an AFM [6]. AFM has become an important tool for the study of cell biology.

AFAM [7], which combines the noninvasive penetration nature of ultrasonic detection and the high-spatial resolution of AFM, has been demonstrated to be able to detect the subsurface structures [8-10] as well as the mechanical properties such as the elastic modulus [11-13] and contact stiffness [14]. It has been used to evaluate the subsurface delamination of chromium (Cr) electrode [15] and nanomechanical characterization of the stiff and soft surfaces

[16]. Striegler et al. [17] reported that the buried void structures could be detected in the thin film of silicon nitride at the depths ranging from 180 to 900 nm and indicate that it depended on the defect dimensions. Zhang et al. used the AFAM for imaging and analyzing the elasticity of vascular smooth muscle cells [18]. In the previous investigations, the cantilever vibrations at ultrasonic frequencies were employed to enhance the AFM cantilever sensitivity to test the sample subsurface structures and mechanical properties. Thus, the approaches are considered as the ultrasonic, acoustic or dynamic method. AFAM not only can observe the surface structure, but also image the subsurface structures.

In this paper, AFM and AFAM images of cells were obtained, respectively. The comparison of the different curing time durations of cells shows that the cells of natural drying without paraformaldehyde were damaged badly. The lamellipodium can be seen for the curing time of 15 minutes with 4% paraformaldehyde.

II. EXPERIMENT

The cells of hepatocyte cell line HL7702 were used in the experiment. The cells were grown in the RPMI-1640 medium (Thermo Scientific Hyclone), and 10% fetal bovine serum (FBS) was added. The environment of the humidified incubator that the cells were cultured was 95% humidity and 5% CO₂ at 37 °C. The cells were cultured on the coverslip (18 × 18 mm). When the cells covered 60%–70% of the cover slip, they were taken out from the culture plates, flushed three times with the phosphate buffer solution (PBS) and then cured with 4% paraformaldehyde for different time durations. Before the experiment the cover slip was flushed three times with PBS and sterile distilled water respectively to remove the paraformaldehyde.

The probe employed was a Tap300AL-G cantilever with a nominal stiffness of 40 N/m and free resonance frequency of 300 KHz. The frequency range employed covers the flexural modes of the cantilever from 10 kHz up to 2 MHz. The contact-resonance frequency of the cantilever and the sample was 38.49 kHz.

III. RESULTS AND DISCUSSIONS

Analysis of the collected images was implemented on the CSPM5500 AFAM system. The AFM and AFAM images of HL7702 cells cured for 0 min are shown in Fig. 1. The

scanning area was $90\mu\text{m} \times 90\mu\text{m}$. The cover slip was naturally dried without paraformaldehyde. The cell membrane was rupturing badly due to the loss of moisture in the naturally-dried case (Fig. 1 (a)).

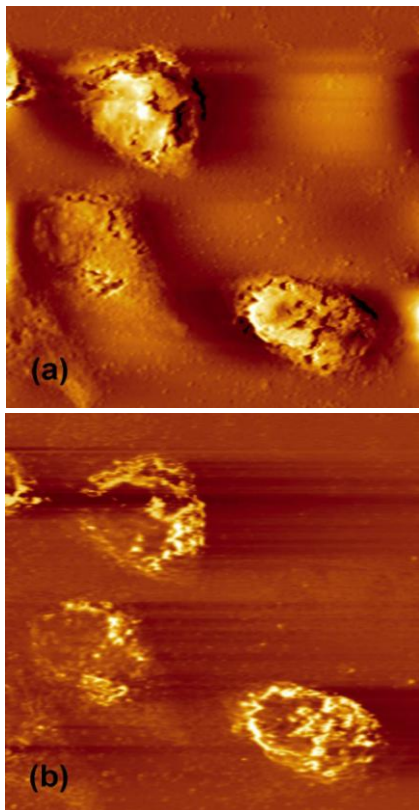


Fig. 1. AFM and AFAM images of HL7702 cells cured for 0 mins. (a) AFM image, and (b) AFAM image.

The topography image maps show differences in the height across the cell surfaces (Fig. 1 (a), Fig. 2 (a), Fig. 3 (a), and Fig. 4 (a)), whereas the acoustic image maps show differences in the elasticity across the surface and subsurface (Fig. 1 (b), Fig. 2 (b), Fig. 3 (b), and Fig. 4 (b)). In the AFM image, the brighter area refers to the larger height [19], whereas the darker area means the smaller height. In the AFAM image, the brighter area refers to larger stiffness, whereas the darker area means the softness [20]. The edge region and center region of the cell are brighter than other regions as shown in Fig. 1 (b). It means the edge region and center region have larger stiffness.

The AFM and AFAM images of HL7702 cells cured for 15 minutes with paraformaldehyde are shown in Fig. 2. The scanning area is $90\mu\text{m} \times 90\mu\text{m}$ in this case. The surfaces of the cells are smooth without any breakage. In Fig. 2, some structures shown in the AFAM image are not present in the AFM image due to the differences of tip-sample interactions. The amplification of the cell center region shows the detail information.

The scanning area of the amplification is $25\mu\text{m} \times 25\mu\text{m}$. The arrows a and b in the AFAM image show the microtubule and the microfilament, respectively. However, the microtubule

and the microfilament are not shown in the same location of the topography. The AFAM images are found with the higher resolution and more information than the AFM images. The lamellipodium can be seen, and the shapes of majority cells are polygonal after curing for 15 minutes. The only way for a cell to move is through the action of the cytoskeleton or the scaffold inside the cell, pushing membrane forward. The cytoskeleton acts as an internal scaffold, made in part of filaments of the protein actin.

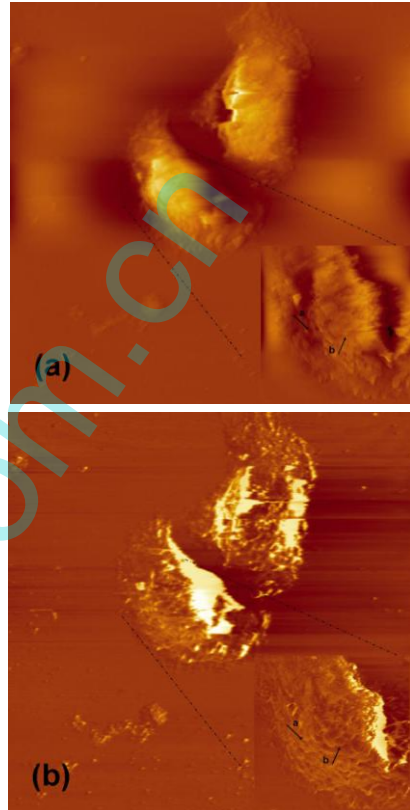


Fig. 2. AFM and AFAM images of HL7702 cells cured for 15 mins. (a) AFM image, and (b) AFAM image.

After curing with paraformaldehyde for 20 minutes (Fig. 3), the lamellipodia was retracted and the cell shape appeared round, and there were some holes appeared on the surface of cytomembrane [21,22]. When the cell was cured for 25 minutes the cytomembrane was pierced and the cytoplasm was spilt out of the cytomembrane, as shown in Fig. 4. The microtubules that the arrow showed formed the cytoskeleton in the cytoplasm in Fig. 4 (b). More information in the cytoplasm was shown from the AFAM image than the AFM image, as well as much better resolution and contrast since more details of cell structures were discernable.

The statistical analysis of the average height of the cells for different curing time durations with 4% paraformaldehyde is shown in Fig. 5. The average height of the cells cured for 15 minutes and 20 minutes show an increasing trend compared with the naturally-dried cells without paraformaldehyde. However, there are no significant variations in the values of

average height between the cells cured for 25 minutes and the naturally-dried cells.

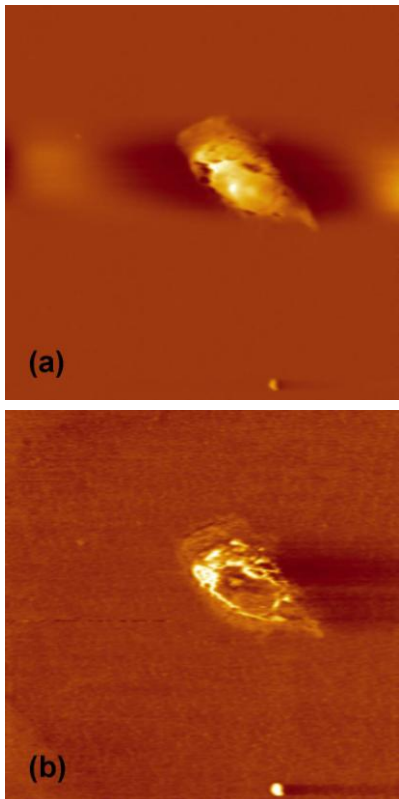


Fig. 3. AFM and AFAM images of HL7702 cells cured for 20 mins. (a) AFM image, and (b) AFAM image.

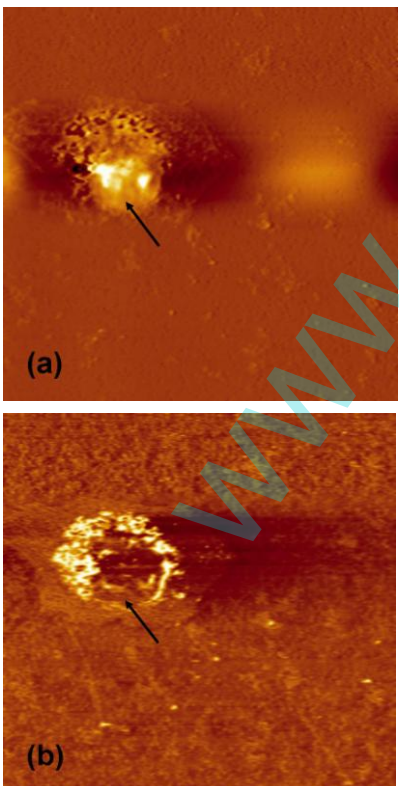


Fig. 4. AFM and AFAM images of HL7702 cells cured for 25 mins. (a) AFM image, and (b) AFAM image.

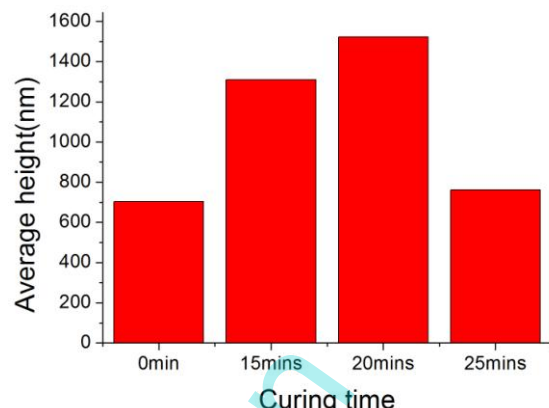


Fig. 5. Statistical analysis of the average height of the cells for different curing time durations with 4% paraformaldehyde.

Fig. 6 shows the statistical analysis of the average surface roughness of the cells for different curing time durations with 4% paraformaldehyde. The average surface roughness values of the cells cured for 15 minutes, 20 minutes and 25 minutes show an increasing trend. In addition, the average surface roughness of the naturally-dried cells without paraformaldehyde is larger than the cured cells with paraformaldehyde.

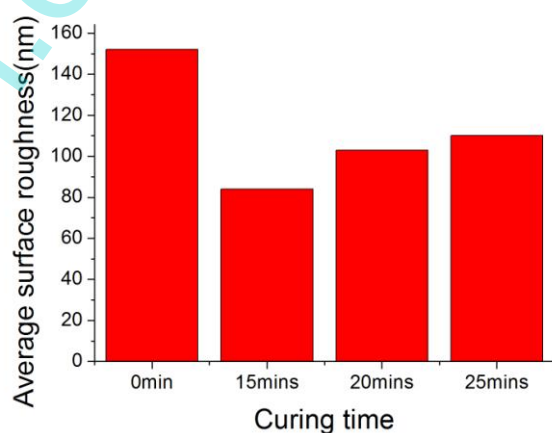


Fig. 6. Statistical analysis of the average surface roughness of the cells for different curing time durations with 4% paraformaldehyde.

IV. CONCLUSION

In this paper, AFM images and AFAM images of cells which were cured with 4% paraformaldehyde for different time durations were obtained, respectively. Comparison of the different curing time durations of cells shows that the naturally-dried cells without paraformaldehyde are damaged badly. The lamellipodium can be seen for the curing time of 15 minutes with 4% paraformaldehyde. After curing with paraformaldehyde for 20 minutes the lamellipodia was retracted and the cell shape appeared round, and there were some holes appeared on the surface of cytomembrane. When

the cell was cured for 25 minutes, the cytomembrane was pierced and the cytoplasm was spilt out of the cytomembrane. Therefore, the optimal curing time was 15 minutes in the experiment. This work provides a method for the study of cured cells in biomedicine.

V. ACKNOWLEDGMENT

This work was supported by EU FP7 (BioRA), EU H2020 (FabSurfWAR), International Science and Technology Cooperation Program of China (No.2012DFA11070), and Jilin Provincial Science and Technology Program (Nos.201215136, 20140414009GH, 20140622009JC, 20140414009GH and 20160623002TC).

REFERENCES

- [1] A. Saraste and K. Pulkki, "Morphologic and biochemical hallmarks of apoptosis", *Cardiovascular Research*, vol. 45, pp. 528–537, 2000.
- [2] T. E. Lister and P. J. Pinhero, "In vivo atomic force microscopy of surface proteins on *Deinococcus radiodurans*", *Langmuir*, vol. 17, pp. 2624-2628, 2001.
- [3] Q. S. Li, G. Y. Lee, C. N. Ong, and C. T. Lim, "AFM indentation study of breast cancer cells", *Biochemical and Biophysical Research Communications*, vol. 374, pp. 609–613, 2008.
- [4] H. Ohshiro, R. Suzuki, T. Furuno and M. Nakanishi, "Atomic force microscopy to study direct neurite-mast cell (RBL) communication in vitro", *Immunology Letters*, vol. 74, pp. 211-214, 2000.
- [5] D. Kirmizis and S. Logothetidis, "Atomic force microscopy probing in the measurement of cell mechanics", *International Journal of Nanomedicine*, vol. 5, pp. 137–145, 2010.
- [6] P. H. Puech, K. Poole, D. Knebel and D. J. Muller, "A new technical approach to quantify cell-cell adhesion forces by AFM", *Ultramicroscopy*, vol. 106, pp. 637-644, 2006.
- [7] U. Rabe, K. Janser and W. Arnold, "Vibrations of free and surface-coupled atomic force microscope cantilevers: Theory and experiment", *Review of Scientific Instruments*, vol. 67, pp. 3281-3293, 1996.
- [8] G. S. Shekhawat, S. Avasthy, A. K. Srivastava and S. H. Tark, "Probing Buried Defects in Extreme Ultraviolet Multilayer Blanks Using Ultrasound Holography", *IEEE Transactions on Nanotechnology*, vol. 9, pp. 671-674, 2010.
- [9] G. S. Shekhawat and V. P. Dravid, "Nanoscale imaging of buried structures via scanning near-field ultrasound holography", *Science*, vol. 310, pp. 89-92, 2005.
- [10] S. Hu, C. Su and W. Arnold, "Imaging of subsurface structures using atomic force acoustic microscopy at GHz frequencies", *Journal of Applied Physics*, vol. 109, pp. 084324-084326, 2011.
- [11] U. Rabe, S. Amelio, M. Kopycinska, S. Hirsekorn and M. Kempf, "Imaging and measurement of local mechanical material properties by atomic force acoustic microscopy", *Surface & Interface Analysis*, vol. 33, pp. 65–70, 2002.
- [12] D. Passeri, A. Bettucci and M. Rossi, "Acoustics and atomic force microscopy for the mechanical characterization of thin films", *Analytical & Bioanalytical Chemistry*, vol. 396, pp. 2769-2783, 2010.
- [13] D. C. Hurley, M. Kopycinskamüller, A. B. Kos and R. H. Geiss, "Nanoscale elastic-property measurements and mapping using atomic force acoustic microscopy methods", *Measurement Science & Technology*, vol. 16, pp. 2167-2172, 2005.
- [14] U. Rabe, S. Amelio, Kester E, V. Scherer, et al. "Quantitative determination of contact stiffness using atomic force acoustic microscopy", *Ultrasonics*, vol. 38, pp. 430-437, 2000.
- [15] K. Yamanaka, K. Kobari and T. Tsuji, "Evaluation of Functional Materials and Devices Using Atomic Force Microscopy with Ultrasonic Measurements", *Japanese Journal of Applied Physics*, vol. 47, pp. 6070-6076, 2008.
- [16] F. Marinello, P. Schiavuta, S. Vezzù, et al. "Atomic force acoustic microscopy for quantitative nanomechanical characterization", *Wear*, vol. 271, pp. 534–538, 2011.
- [17] A. Striegler, B. Koehler, B. Bendjus, et al. "Detection of buried reference structures by use of atomic force acoustic microscopy", *Ultramicroscopy*, vol. 111, pp. 1405-1416, 2011.
- [18] B. Zhang, Q. Cheng, M. Chen, et al. "Imaging and Analyzing the Elasticity of Vascular Smooth Muscle Cells by Atomic Force Acoustic Microscope", *Ultrasound in Medicine & Biology*, vol. 38, pp. 1383-1390, 2012.
- [19] H. J. Butt, E. K. Wolff, S. A. C. Gould, et al. "Imaging cells with atomic force microscope", *Struct Biol*, vol. 105, pp. 54-61, 1990.
- [20] X. Chen, X. Fang and J. Song, "Design and manufacturing of scanning probe acoustic microscope test phantom", *Proceedings of Spie*, vol. 9419, pp. 94190A-8, 2015.
- [21] N. A. Amro, L. P. Kotra, K. Wadu-Mesthrige, et al. "High-resolution atomic force microscopy studies of the *Escherichia coli* outer membrane: Structural basis for permeability", *Langmuir*, vol. 16, pp. 2789-2796, 2000.
- [22] B. N. Mason, J. P. Califano and C. A. Reinhart-King, "Matrix Stiffness: A Regulator of Cellular Behavior and Tissue Formation", *Engineering Biomaterials for Regenerative Medicine*, pp. 19-37, 2012.